Solid particle erosion of unidirectional carbon fibre reinforced polyetheretherketone composites

U.S. Tewari[a,*], A.P. Harsha[a], A.M. Hãger[b], K. Friedrich[b]

[a] *Industrial Tribology, Machine Dynamics and Maintenance Engineering Centre, Indian Institute of Technology, Hauz Khas, New Delhi 110 016, India*
[b] *Institute for Composite Materials, University ofKaiserlautern, Kaiserlautern, Germany*

Received 24 September 2001; received in revised form 20 March 2002; accepted 12 April 2002

Abstract

The solid particle erosion behaviour of unidirectional carbon fibre (CF) reinforced polyetheretherketone (PEEK) composites has been characterised. The erosion rates of these composites have been evaluated at different impingement angles (15-90°) and at three different fibre orientations (0, 45, and 90°). The particles used for the erosion measurements were steel balls with diameter of 300-500 (xm and impact velocities of 45 and 85 m/s. The unidirectional CF reinforced PEEK composites showed semi-ductile erosion behaviour, with maximum erosion rate at 60° impingement angle. The fibre orientations had a significant influence on erosion rate. The morphology of eroded surfaces was examined by using scanning electron microscopy (SEM). Possible erosion mechanisms are discussed.

Keywords: Solid particle erosion; Polyetheretherketone (PEEK); Composites; Carbon fibres; Fibre orientations

1. Introduction

Polymer composite materials have generated wide interest in various engineering fields, particularly in aerospace applications, because they exhibit, high specific strength and stiffness as compared to monolithic metal alloys. Polymer composite materials are therefore, finding increased application under conditions in which they may be subjected to solid particle erosion. Examples of such applications are pipe line carrying sand slurries in petroleum refining, helicopter rotor blades [1,2], pump impeller blades, high speed vehicles and aircraft operating in desert environments, water turbines, aircraft engine blades [3]. However, polymer composite materials exhibit poor erosion resistance as compared to metallic materials [4]. It is also known that the erosive wear of polymer composites is usually higher than that of the unreinforced polymer matrix [5].

Many researchers [1-24,29] have evaluated the resistance of various types of polymers and their composites to solid particle erosion. Materials that have been eroded include nylon [6,7], epoxy [19-21], polypropylene [13,16] polyethylene [14], polyetheretherketone (PEEK) [15,18] UHMWPE [29] and various polymer based composites [1,4,5,8-10,17-20,22]. The majority of studies have used either quartz particles or spherical balls.

Erosive wear resistance of polymers and their composites is therefore, of substantial interest. However, a comprehensive and systematic study of erosion of unidirectional carbon fibre (CF) reinforced PEEK composites has not previously been performed. Unidirectionally reinforced fibre composites represent the basic element of complex composite structures. Therefore, study of their behaviour is an important component of the analysis of erosive wear of polymer composites. The objective of the present investigation was to study the solid particle erosion characteristics of unidirectional CF reinforced PEEK composites under various experimental conditions. Another aim was to study the effect of relative fibre orientation on erosive wear behaviour. In the present study steel balls of 300-500 (xm were used as erodent. In most practical situations erosive wear particles are irregular dust grains of much lower density than steel. The steel balls were used because it implies higher energy by single impact. The present testing condition was used, even though it is unusual, because the objective was to carry out a fundamental study of erosion and to investigate the effect of fibre orientation in composites on steel ball impact.

2. Experimental details

2.1. Materials

Unidirectional CF reinforced PEEK composites were manufactured from non-woven fabric NCS-1057 (BASF) made from Celion G30-500 CFs commingled with PEEK (150 G) filaments [25]. A commingled system consists of hybrid yarns of intimate blend of continuous thermoplastic filaments and reinforcing fibres. Composites were compression moulded in a laboratory press. A number of 10 cm x 16 cm panels consisting of 16 unidirectional plies were manufactured. The mould was heated to 410 °C in about 5 min and held at this temperature for 20 min. A pressure of 25 bar was then applied for 30 min and the mould was cooled to 70 °C by circulating water in about 10 min. From these moulded plates test samples of approximately of 30 mm x 30 mm x 3 mm in dimension were cut using a diamond cutter. The composites were characterised by various analytical methods. Glass transition temperature (T_g), melting temperature (T_m) and crystallinity were measured by using differential scanning calorimeter (DSC Mettler Thermal Analyser) at heating rate of 10°C/min, in N2 atmosphere to prevent oxidation of the specimen. The degree of crystallinity of the composites was calculated from the melting peaks in the DSC scan. The heat of post curing was subtracted. The heat of fusion of fully crystalline PEEK is 130 Jg^{-1} [26]. The fibre volume fraction was measured by density measurements. The densities of the composites were measured by weighing samples in ethanol. The fibre volume fraction was then calculated from known densities of components. The densities of PEEK and the fibres were 1.33 and 1.75g/cm^3, respectively. The hardness (H_v) of the composites was obtained at 1 kg load by using a Vickers hardness tester. Table 1 provides the properties of the unidirectional CF reinforced PEEK composites.

2.2. Erosive wear test rig

The room temperature erosion test facility used in the present investigation is illustrated schematically in Fig. 1. The particles are driven by a static pressure P and are accelerated along an 80 mm long nozzle of 8 mm diameter. The velocity of the eroding particles is determined using the rotating disc method [27]. The distribution of average particle velocities and mass flow throughout the flow cross-section were obtained for several values of pressure P at various distances from the nozzle tip. It was found that the average velocity at higher pressures is rather uniformly distributed within a 15 mm distance around the flow axis. However, the mass flow decreases substantially with distance from the flow axis. Pressures of 4 and 8bar were used in erosion testing. The average velocities of the steel balls at these pressures at 160 mm from nozzle tip were 45 and 85 m/s, respectively. Then mounted specimens were subjected to a particle flow at a given impingement angle and angle of fibre orientation (Fig. 2). Wear was measured by weight loss after each 15 s of erosion. Samples of 30 mmx 30 mmx 3 mm were cut from the composites and mounted in the specimen holder

Table 1
Properties of the carbon fibre reinforced PEEK composites used

Glass transition temperature, T_g (°C)	131
Melting temperature, T_m (°C)	342
Crystallinity (%)	28
Density (g/cm^3)	1.60
Fibre volume fraction (*Vf* (%))	65
Vickers hardness H_v (kg/cm^2)	42.1

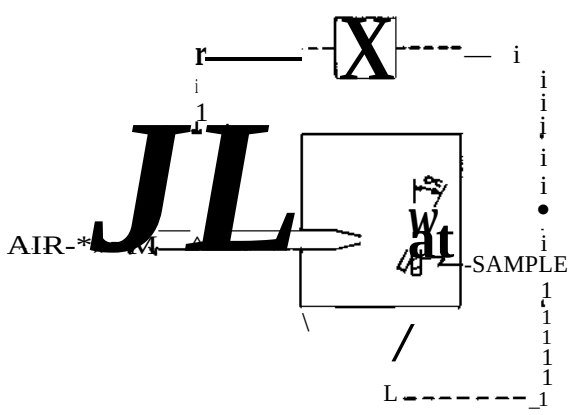

Fig. 1. Schematic diagram of erosion rig.

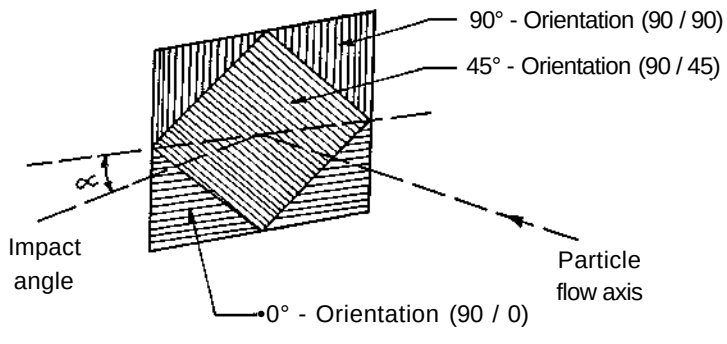

Fig. 2. Definition of impingement angle and fibre orientation.

Table 2
Erosion test conditions

Test parameters	
Erodent	Steel balls
Erodent size *(\xm)*	300-500
Erodent shape	Round
Vickers hardness of erodent, H_v (kg/cm^2)	400-800
Density of steel ball (g/cm^3)	7.8
Impingement angles	15-90°
Impact velocities (m/s)	45 ± 5, 85 ± 5
Fibre orientations	0° (90/0), 45° (90/45), 90° (90/90)
Erodent feed rate (g/s)	15
Test temperature	RT
Nozzle to sample distance (mm)	160

by 2 mm thick steel cover plate with a hole of 30 mm in diameter. The conditions under which the erosion tests were carried out are listed in Table 2.

2.3. Characterization of eroded samples

To characterise the morphology of the eroded surfaces and to understand the mode of material removal, the eroded samples were observed using a scanning electron microscope (S 600, Cambridge). The samples were gold sputtered in order to reduce charging of the surface.

3. Results and discussion

The weight loss of CF reinforced PEEK as a function of mass of erodent at an impingement angle of 60° for different three fibre orientations is shown in Fig. 3 a and b. Fig. 4a and b shows the variation of the normalised erosion rate with impingement angle for three different fibre orientations. Scanning electron microscopy (SEM) micrographs of worn samples are shown in Figs. 6-7.

3.1. Effect of Impingement angle

Fig. 3a and b shows typical curves of weight loss as a function of mass of erodent at an impingement angle of 60° for different impact velocities. The curve shows a steady state is reached, in which weight loss is proportional to the mass of erodent that has impacted on the specimen. An incubation period was not observed in these cases. Erosion rates were calculated by dividing the weight loss of specimen by the mass of erodent that impacted.

Fig. 4a and b shows the influence of impingement angle and impact velocity on the erosion rate of CF reinforced PEEK. It can be seen that the erosion rate was a maximum at 60° impingement angle for all fibre orientations. This is semi-ductile erosion behaviour. The erosion rate was almost doubled when impact velocity is increased to 85 m/s. The shapes of the curves are similar in both cases. The effect of

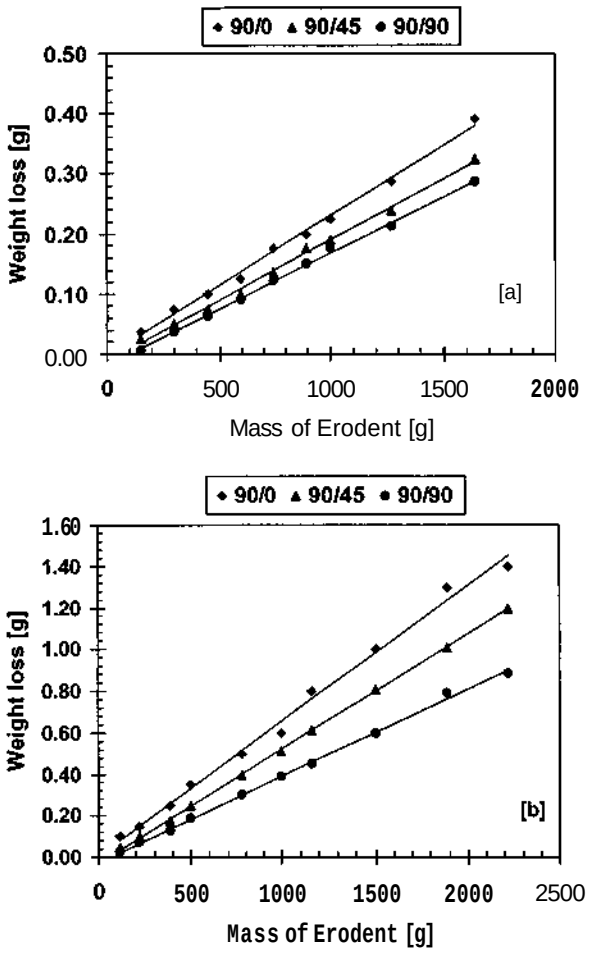

Fig. 3. Variation of erosive wear with mass of erodent for different impact velocity *(V):* (a) 45 m/s; (b) 85 m/s; (impingement angle = 60°; exposure time = 180 s).

fibre orientation is more pronounced at the higher impingement angle. The order of performance at 60° impingement angle was 90/0 (0° fibre orientation) >90/45 (45° fibre orientation) >90/90 (90° fibre orientation).

The most important factors influencing the erosion rate of materials are the impact velocity, impact angle of the erodent particles, the size, shape and hardness of eroding particles [28]. Table 3 provide details of erosion experiments carried out by various investigators. Many investigators have used angular silica sand, alumina, corundum particles or irregular silicon carbide (SiC) abrasives. In the present study steel balls were used as erodent. Hence, it is difficult to compare present erosion data precisely with literature data. Tilly and Sage [7] investigated the influence of velocity, impingement angle, particle size and weight of impacted abrasive for nylon, CF reinforced nylon, and epoxy (EP) resin, polypropylene and glass fibre (GF) reinforced plastic. There results showed that, for particular materials and conditions of their test, composite materials generally behaved in an ideally brittle fashion (i.e. maximum erosion rate occurred at normal impact). Miyazaki

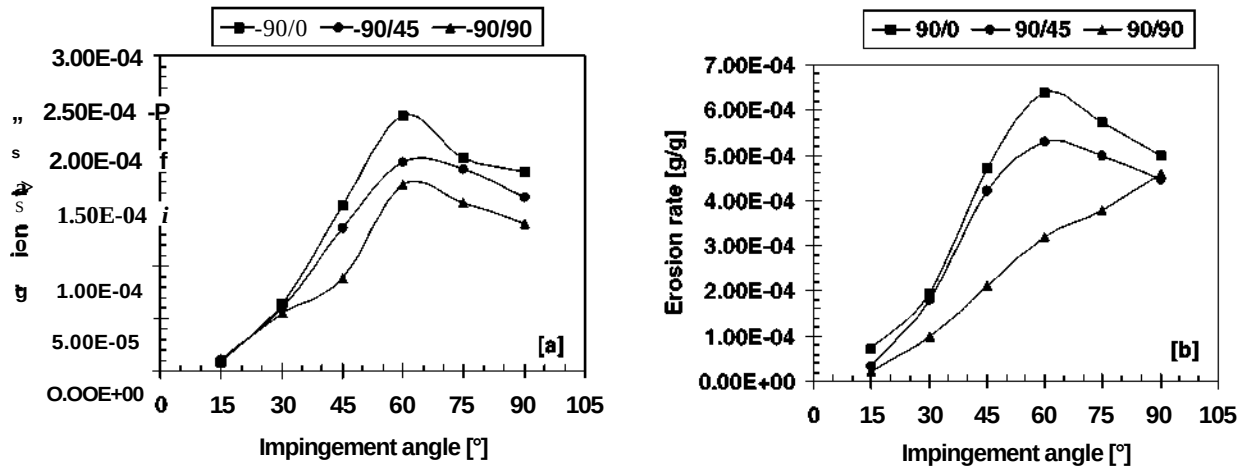

Fig. 4. Variation of normalised erosion rate with impingement angle for three fibre orientations: (a) impact velocity *(V)* 45m/s; (b) 85m/s (exposure time = 180 s).

and Hamao [18] carried out experiments to study the effect of matrix material, reinforcement of short carbon and GFs, impingement angle, and particle velocity on the solid particle erosion behaviour of PEEK resin. It was observed that PEEK and its composites show maximum erosion rate at a low impingement angle of 30°. The particles used were SiC abrasives with particle diameters ranging from 100 to 150 (xm. Häger et al. [5] conducted erosion tests on GF/EP, CF/EP, CF reinforced PEEK, CF/ polyetherketoneketone (PEKK), and aramid fibre (AF) reinforced EP (AF/EP). The authors claimed a semi-ductile behaviour of both thermoset and thermoplastic composites under jet erosion by corundum particles. The maximum erosion rate was observed at an angle of impingement of 60° for all the materials tested except AF/EP. Zahavi and Schmitt [8] came to a similar conclusion for the case of E-glass/EP composites. The erodent medium in the study was natural sand of between 210 and 297 (im size. Manish Roy et al. [4] concluded

Table 3
Details of erosion experiments carried out on polymer/polymer matrix composites by various investigators

Material tested	Test conditions	Type of erodent, shape and size used	Reference
Glass epoxy resin, glass phenolic resin (modified), glass phenolic resin (unmodified) and glass polyester resin	V = 38 ± 5, 45 ± 5 m/s; α = 30, 90°	Silica sand, angular, 200 ± 50 [xm	[4]
Unidirectional glass, carbon and aramid reinforced composites with epoxy PEEK and PEEK matrix	V = 85 m/s; α =15, 30, 60, 90°	Corundum particles, angular, 400 [xm	[5]
Quartz polybutadiene, glass cloth epoxy and quartz polyimide composites	V =42 m/s; α = 30, 45, 60, 75, 90°	Natural sea sand, slightly rounded, 210-297 [xm	[8]
Bismaleimide (BMI) matrix and reinforced with graphite fibre	K = 20, 40, 60 m/s; a =30, 90°	Alumina oxide particles, angular, 63, 130 and 390 [xm	[10]
Bismaleimide (BMI) matrix	K = 60m/s; α =90°	Alumina oxide particles, angular, 42, 63, 143 and 390 [xm	[11]
Polystyrene, polyethylene, polypropylene, polybutene	V = 57 m/s; a = 90°; room temperature and — 35 °C	Steel balls, spherical, diameter of 500 [xm	[12]
Nylon 66, nylon 6, ABS reinforced with short glass, carbon fibres, thermoset resin unsaturated polyester and epoxy reinforced by woven glass cloth	K = 23, 29, 35, 47m/s; a = 15, 30, 45, 60, 90°	SiC abrasives, irregular, 100-150 [xm	[17]
Thermoplastic polyimide, PEEK matrix and reinforced with glass, carbon fibres	V= 17,34, 56.7m/s;α = 15, 30, 45, 60, 90°	SiC abrasives, irregular, 100-150 [xm	[18]
Epoxy and reinforced with unidirectional carbon fibres	V = 18.9, 34.6, 55.7m/s; a = 15, 30, 45, 60, 90°	SiC abrasives, irregular, 100-150 [xm	[19]
Epoxy matrix and reinforced with unidirectional glass fibre	K = 70m/s; α =30, 60, 90°	Corundum particles, angular, 60-120 [xm	[20]
Ultra high molecular weight polyethylene (UHMWPE)	V = 10, 20, 40, 70, 100 m/s; a = 15, 30, 45, 60, 75, 90°	Coal powder, silicon dioxide, angular, 60-70 mesh size	[29]

V, impact velocity (m/s); α, impact angle (°).

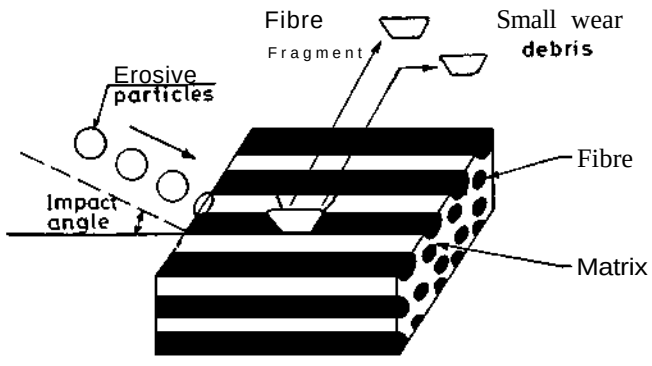

(a) Parallel impact [90°-Orientation (90/90)]

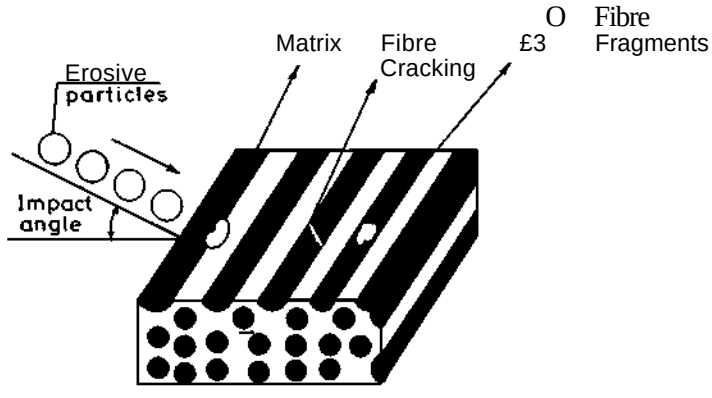

(b) Perpendicular impact [0°-Orientation (90/0)].

Fig. 5. Schematic diagrams of erosive process in unidirectional fibre reinforced composites under parallel and perpendicular impact conditions.

that composites with a thermoset matrix (EP and phenolic) behave in brittle manner while the composites with a thermoplastic matrix (polyester) responded in a ductile fashion.

In the erosion tests, plastics show ductile nature, and it is known [30,31] that ductile materials have a peak erosion rate around 30° because cutting mechanism is dominant in erosion. Also Miyazaki and Hamao [18] reported peak erosion rate for unreinforced PEEK matrix is around 30°. A possible reason for the erosion behaviour in the present study is that the CFs used as reinforcement for the PEEK matrix are a typical brittle material, so that erosion is mainly caused by damage mechanisms as micro-cracking or plastic deformation due to the impact of steel balls. Such damage is supposed to increase with the increase of kinetic energy loss. According to Hutchings et al. [32], kinetic energy loss is a maximum at an impingement angle of 90°, where erosion rates are maximum for brittle materials. In the present study also, the peak erosion rate shifts to a larger value of impingement angle due to the brittle nature of CFs.

3.2. Effect of fibre orientation

The effect of fibre orientation on erosive wear of polymer composites has been studied to limited extent [1,5,9,10,19,20]. Earlier, investigators [1,5] observed anisotropy in the erosion behaviour of reinforced composites and pointed out the clear dependence of erosion rate on fibre orientations. Carbon fibre reinforced PEEK composites showed higher erosion rates in the 90/0 (0° fibre orientation) as compared to 90/45 (45° fibre orientation) and 90/90 (90° fibre orientation), especially at 60° impingement angle. These results are in agreement with some previous observations [1,5,10,19,20] but in disagreement with others [9]. It is well known that fibres in composites, subjected to particle flow, break in bending [1]. Fig. 5 shows a schematic diagram of erosive wear processes in unidirectional reinforced composites at different fibre orientations. In the case of an impact having a parallel component of the velocity with respect to the fibre orientation, bending requires particle indentation of the composites. Indentation involves compressive stresses and the resistance to micro bending is very high. It is quite clear from the diagram that, under parallel impact, when the matrix material is removed, the steel balls hits the fibre directly and thus the interface between fibre and matrix becomes less dominant (Fig. 5a). In case of perpendicular impact, the resistance to the lateral component of bending moment is lower and bundles of fibres get bent and broken more easily. This results in an increase in

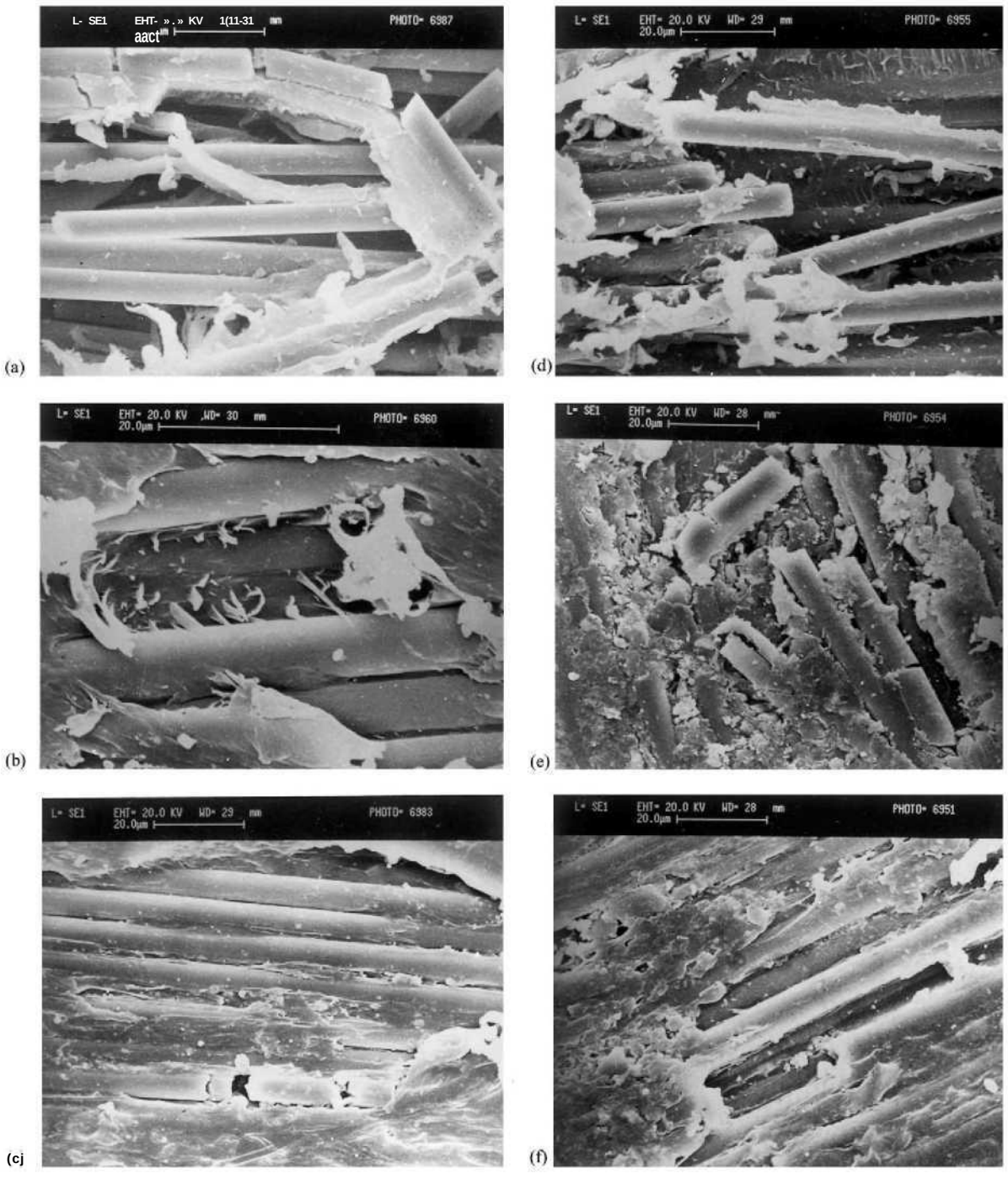

Fig. 6. Scanning electron micrograph of surfaces eroded at impingement angle of 15° with steel balls of diameter 300-500 [xm. Impact velocity is 45 m/s for (a-c) and 85 m/s for (d-f), respectively ((a) and (d) 90/0-0° fibre orientation; (b) and (e) 90/45-45° fibre orientation; (c) and (f) 90/90-90° fibre orientation).

erosive wear (Fig. 5b). Similarly in the case of 45° fibre orientation, the fibres are more prone to bend and break easily.

4. Surface morphology of eroded surface

Fig. 4a and b show that erosion rate was a maximum at 60° and a minimum at 15° impingement angles for all three fibre orientations at impact velocity of 45 and 85 m/s. These eroded surfaces were examined by using SEM and the results are shown in Figs. 6-7.

Fig. 6 shows a SEM of surfaces eroded at an impingement angle of 15° at different impact velocities and three fibre orientations. Fig. 6a and d show the surfaces with fibres oriented perpendicular to the direction of the steel ball impacts. It is seen from the micrograph that transverse particle flow

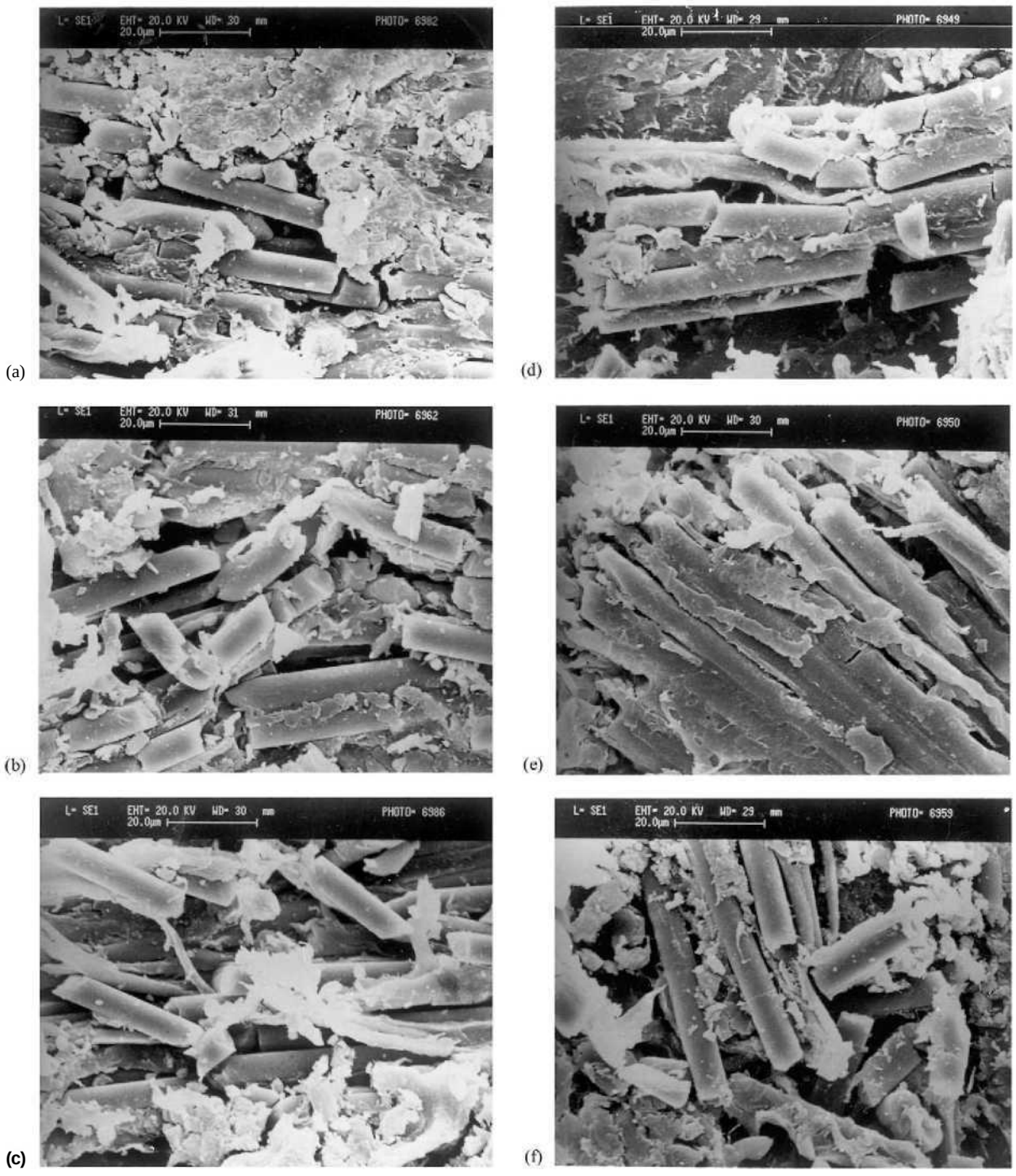

Fig. 7. Scanning electron micrograph of surfaces eroded at impingement angle of 60° with steel balls of diameter 300-500 *ixn*. Impact velocity is 45 m/s for (a-c) and 85 m/s for (d-f), respectively ((a) and (d) 90/0-0° fibre orientation; (b) and (e) 90/45-45° fibre orientation; (c) and (f) 90/90-90° fibre orientation).

creates bending of fibres, fibre cracking and subsequent fibre removal. Some of the bent fibres are broken but not removed due to their good adhesion. Figs. 6c and f show a portion of the eroded surfaces with fibres parallel to the direction of steel ball impact. The matrix covering the fibre seems to be chipped off and the crater thus formed shows an array of almost intact fibres. In the case of parallel erosion, bending of fibres associated with indentation is limited. Figs. 6b and e show surfaces with fibres oriented at 45° to the direction of steel ball impact. There is local removal of matrix material from the impact surfaces resulting in exposure of fibres to the erosive environment. The fibres are still held firmly in place as yet by the undamaged matrix material surrounding them.

Fig. 7 shows a scanning electron micrograph of surfaces eroded at an impingement angle of 60° at different impact velocities and three fibre orientations. Figs. 7a and d show surfaces with fibres oriented perpendicular to the direction of steel ball impact. The micrographs show that bundles of bent CFs embedded in plastically deformed matrix. The steel ball impacts on the fibres cause the fibres to break owing to the formation of cracks perpendicular to their length. Some of the bent fibres are broken but not removed due to their good adhesion. Transverse erosion causes a lateral bending moment and fibres are more easily bent and broken. In the case of parallel erosion (Fig. 7c and f) the many broken fibre fragments are mixed with the matrix microflake debris. It is also seen that fibres protruded out of the matrix phase. The damage was characterised by the separation and detachment of broken fibres from the matrix. Fig. 7b and e show the surfaces with fibres oriented at 45° to the direction of steel ball impact. Wavy fibre pattern is observed, the fibres being almost intact, the broken fibre fragments being often bonded to the matrix (Fig. 7e). The matrix covering the fibres was almost removed, broken fibres of comparatively large size were dispersed in various directions on the surface (Fig. 7b). The higher matrix toughness allows substantial plastic deformation, which absorbs large amount of the impact energy.

5. Conclusions

Based on this study of the solid particle erosion of unidirectional CF reinforced PEEK composites at various impingement angles, impact velocities and three fibre orientations the following conclusions can be drawn:

1. The composites exhibited a maximum erosion rate at an impingement angle of 60° under the present experimental condition.
2. The fibre orientation has a significant influence on the erosion rate of composites. The erosion rate is higher when the balls impact on fibres normally than the ball impacts the composite in a direction parallel to the fibres. The degree of fibre breakage appears to vary with fibre orientation.
3. The morphologies of eroded surfaces observed by SEM suggest that the overall erosion damage of composites consists of matrix removal and exposure of fibres, fibre cracking and removal of broken fibres.

Acknowledgements

One of the author (UST) thanks the German Academic Exchange Services, BONN, (Germany), for financial assistance and Director, Institute for Composite Materials, University of Kaiserlautern, Kaiserlautern, (Germany) for allowing to use the facilities during this work.

References

[1] K.V. Pool, C.K.H. Dharan, I. Finnie, Erosive wear of composite materials, Wear 107 (1986) 1-12.
[2] S.M. Kulkarni, Kishore, Influence of matrix modification on the solid particle erosion of glass/epoxy composites, Polym. Polym. Composites 9 (2001) 25-30.
[3] H.A. Aglan, T.A. Chenock Jr., Erosion damage features of polyimide thermoset composites, SAMPEQ (1993) 41-47.
[4] M. Roy, B. Vishwanathan, G. Sundararajan, The solid particle erosion of polymer matrix composites, Wear 171 (1994) 149-161.
[5] A. Hãger, K. Friedrich, Y.A. Dzenis, S.A. Paipetis, Study of erosion wear of advanced polymer composites, in: K. Street, B.C. Whistler (Eds.), Proceedings of the ICCM-10, Canada Woodhead Publishing Ltd., Cambridge, 1995, pp. 155-162.
[6] G.P. Tilly, Erosion caused by airborne particles, Wear 14 (1969) 63-79.
[7] G.P. Tilly, W. Sage, The interaction of particle and material behaviour in erosion process, Wear 16 (1970) 447-465.
[8] J. Zahavi, G.F. Schmitt Jr., Solid particle erosion of reinforced composite materials, Wear 71 (1981) 179-190.
[9] T.H. Tsiang, Sand erosion of fibre composites: testing and evaluation, in test methods for design allowables for fibrous composites, in: C.C. Chamis (Ed.), ASTM STP 1003, American Society for Testing and Materials, Vol. 2, Philadelphia, PA, 1989, p. 55.
[10] P.J. Mathias, W. Wu, K.C. Goretta, J.L. Routbort, D.P. Groppi, K.R. Karasek, Solid particle erosion of a graphite fibre reinforced bismaleimide polymer composite, Wear 135 (1989) 161-169.
[11] A. Brandstader, K.C. Goretta, J.L. Routbort, D.R. Groppi, K.R. Karasek, Solid particle erosion of bismaleimide polymers, Wear 147 (1991) 155-164.
[12] K. Friedrich, Erosive wear of polymer surfaces by steel blasting, J. Mat. Sci. 21 (1986) 3317-3332.
[13] S.M. Walley, J.E. Field, I.M. Scullion, F.P.M. Heukensfeldt Jansen, D. Bell, Dynamic strength properties and solid particle erosion behaviour of a range of polymers, in: J.E. Field, J.P. Dear (Eds.), Proceedings of the 7th International Conference on Erosion by Liquid and Solid Impact, Cavendish Laboratory, Cambridge, 1984, p. 59.
[14] S.M. Walley, J.E. Field, The erosion and deformation of polyethylene by solid particle impact, Phil. Trans. Roy. Soc., Lond. A 321 (1987) 277-303.
[15] S.M. Walley, J.E. Field, M. Greengrass, An impact and erosion study of PEEK, Wear 114 (1987) 59-71.
[16] S.M. Walley, J.E. Field, P. Yennadhiou, Single solid particle impact erosion damage on polypropylene, Wear 100 (1984) 263-280.
[17] N. Miyazaki, N. Takeda, Solid particle erosion of fibre reinforced plastics, J. Comp. Mater. 27 (1993) 21-31.
[18] N. Miyazaki, T. Hamao, Solid particle erosion of thermoplastic resins reinforced by short fibres, J. Comp. Mater. 28 (1994) 871-883.
[19] N. Miyazaki, T. Hamao, Effect of interfacial strength on erosion behaviour of FRPs, J. Comp. Mater. 30 (1996) 35-50.
[20] N.M. Barkoula, J. Karger-Kocsis, Solid particle erosion of unidirectional GF reinforced EP composites with different fibre/matrix adhesion, J. Reinforced Plast. Composites 19 (2000) 1-12.
[21] N.M. Barkoula, J. Gremmels, J. Karger-Kocsis, Dependence of solid particle erosion on the cross-link density in an epoxy resin modified by hygrothermally decomposed polyurethane, Wear 247 (2001) 100-108.
[22] K.R. Karasek, K.C. Goretta, D.A. Helberg, J.L. Routbort, Erosion in bismaleimide polymers and bismaleimide polymer composites, J. Mater. Sci. Lett. 11 (1992) 1143-1144.
[23] P.V. Rao, D.H. Buckley, Angular particle impingement studies of thermoplastic materials at normal incidence, ASLE Trans. 29 (1986) 283-298.
[24] P.V. Rao, S.G. Young, D.H. Buckley, Solid Spherical Glass Particle Impingement Studies of Plastic Materials, National Aeronautics and Space Administration, Report no. NASA-TP-2161, 1983.

[25] T.V. Khanh, J. Denault, Effect of moulding parameters on the interfacial strength in PEEK/carbon composites, J. Reinforced Plast. Composites 12 (1993) 916-931.
[26] D.C. Bassett, R.H. Olley, I.A.M. Al Raheil, On crystallisation phenomena in PEEK, Polymer 29 (1988) 1745-1754.
[27] A.W. Ruff, L.K. Ives, Measurement of solid particle velocity in erosive wear, Wear 35 (1975) 195-199.
[28] J.C. Arnold, I.M. Hutchings, The erosive wear of elastomers, J. Nat. Rubb. Res. 6 (1991) 241-256.
[29] Y.Q. Wang, L.P. Huang, W.L. Liu, J. Li, The blast erosion behaviour of ultrahigh molecular weight polyethylene, Wear 218 (1998) 128—133.
[30] J.G.A. Bitter, A study of erosion phenomenon. Part I, Wear 13 (1963) 5-21.
[31] J.G.A. Bitter, A study of erosion phenomenon. Part II, Wear 13 (1963) 169-190.
[32] I.M. Hutchings, R.E. Winter, J.E. Field, Solid particle erosion of metals: the removal of surface material by spherical projectiles, Proc. Roy. Soc. Lond., Ser. A 348 (1976) 379-392.